JOURNAL OF THERMOPHYSICS AND HEAT TRANSFER
Vol. 6, No. 3, July–Sept. 1992

Laminar Heat Transfer to Blunt Cones in High-Enthalpy Hypervelocity Flows

S. L. Gai*
University College, University of New South Wales, Canberra, ACT 2600 Australia
and
W. S. Joe†
Australian National University, Canberra, ACT 2600 Australia

Measurements of heat transfer on spherically blunted cones of various bluntness ratios in high-enthalpy hypervelocity air flows obtained using a free-piston-driven shock tunnel are described. The stagnation enthalpies considered were in the range 14--20-MJ/kg (equivalent to flight speeds 4--6-km/s). The corresponding equilibrium stagnation temperatures were in the range 7000–9000 K. Comparison of measured data showed reasonable agreement with the classical theory of Lees[1] for small bluntness ratios while the large bluntness ratio results compared well with the empirical theory of Griffith and Lewis.[4]

Nomenclature

C = correlation constant in Griffith & Lewis' empirical relation, Eq. (4)
C_p = pressure coefficient, $(p_w - p_\infty)1/2\rho_\infty U_\infty^2$
c = specific heat capacity
d = nose diameter, mm
h = enthalpy, MJ/kg
K = constant in Eq. (2)
k = nose drag coefficient or thermal conductivity
L = axial length from tip of nose to base, mm
M = Mach number
p = pressure
$\dot{q}_0$ = stagnation heat transfer on the nose, Eq. (3)
$\dot{q}_s$ = computed stagnation heat transfer of a sphere, Eq. (2)
$\dot{q}_w$ = surface heat transfer on the cone, MW/m^2
R_B = base radius, mm
Re = Reynolds number
R_N = nose radius, mm
s' = distance along the cone surface from virtual tip, Eq. (3) and Fig. 1
T = temperature, K
t = time, s
U = velocity, km/s
x = distance measured axially from the base, Fig. 1, mm
x' = distance measured axially from the nose tip, Fig. 1, mm
γ = specific heat ratio
ε = normal shock density ratio
θ_c = cone half angle
ρ = density, kg/m^3

Subscripts
∞ = freestream conditions
0 = reservoir/stagnation conditions
0′ = reservoir/stagnation conditions behind normal shock
f = frozen conditions
r = recovery value
t_2 = pitot pressure behind normal shock
w = wall/surface conditions

Received March 19, 1990; revision received Dec. 7, 1990; accepted for publication Dec. 13, 1990.

*Senior Lecturer, Department of Mechanical Engineering Australian Defence Academy. Associate Fellow AIAA.
†Research Assistant, Department of Physics, Faculties.

Introduction

THERE has been a resurgence of interest in the study of aerothermodynamic problems of hypervelocity flight with the proposed plans for building reusable spaceplanes and aero-assisted orbital transfer vehicles (AOTVs). This new generation of spacecraft will be subjected to prolonged radiative and convective heating during their trajectory through low-density upper atmosphere at speeds ranging from 5 km/s to 10 km/s. It is important, therefore, to understand the physical and chemical gas dynamic processes in the flow over such vehicle configurations, especially in the forebody regions. A simple forebody configuration amenable to both theoretical and experimental studies is a spherically blunted cone.

Flow around sphere cones has been studied for a long time.[1–3] In particular, there are a number of studies dealing with laminar heat transfer measurements at hypersonic speeds.[4–6] The present paper reports an investigation of flow over blunt cones with emphasis on heat transfer under flow conditions that are typical of re-entry. All the spacecraft designs presently under consideration, such as AOTV, NASP (U.S.A.), HOTOL (U.K.), and Hermes (France) have blunt-nosed shapes. The stagnation enthalpy range considered was 14–20 MJ/kg giving equivalent re-entry speeds in the range 4–6 km/s. The corresponding equilibrium stagnation temperatures were in the range 7000–9000 K.

Facility and Experimental Conditions

The tests were conducted at the Australian National University free-piston-driven shock tunnel T3 with air as test gas and helium as driver gas. The flow was generated through a conical nozzle of 305-mm exit diameter and 12.7-mm throat. This provided a test gas of frozen composition at a Mach number of about 7.8. The tunnel was operated at two different conditions. These conditions are designated as run types B and D and were typical of high (H) and medium (M) enthalpy flow respectively. Thus, at condition B, most of the oxygen and a small fraction of nitrogen is dissociated into oxygen and nitrogen atoms. At condition D, nearly two-thirds of the oxygen but no nitrogen was dissociated. The full details of the flow at these conditions are shown in Table 1.

Table 1 Freestream conditions at the exit plane of the nozzle

	Reservoir conditions					Freestream conditions				
Run type	Stagn. press. p_0, atm	Stagn. enthalpy h_0, MJ/kg	Equilib. stagn. temp. T_0, K	Wall to Stagn. temp. ratio T_w/T_0	Velocity U_∞, km/s	Density $\rho_\infty \times 10^3$ kg/m^3	Temp. T_∞, K	M_∞	γf	Re_∞/mt
B(H)	260	19.8	8645	0.0347	5.6	2.37	1140	7.8	1.45	29.5×10^4
D(M)	210	13.6	7178	0.0418	4.7	2.65	870	7.7	1.43	33×10^4

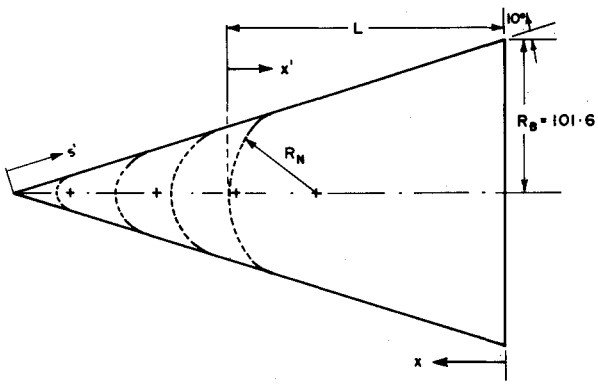

Fig. 1 Blunt cone model. (All dimensions in mm.)

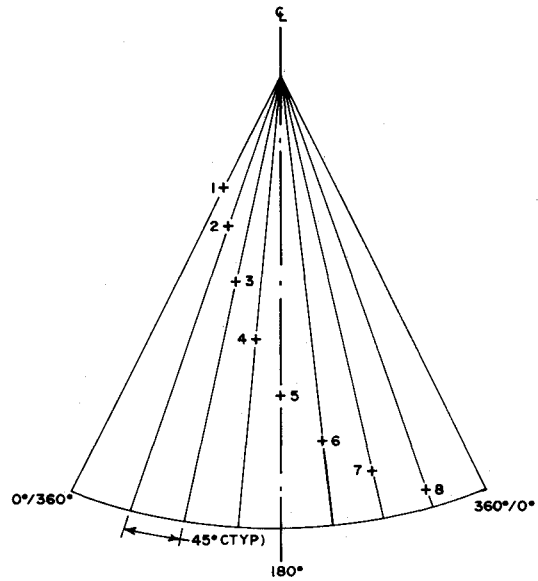

Fig. 2 Thermocouple locations on the cone surface.

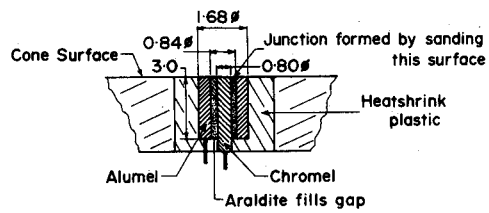

Fig. 3 Thermocouple assembly showing details. (All dimensions in mm.)

The freestream conditions at the exit plane of the nozzle were obtained, first by calculating the nozzle reservoir conditions from the measured shock speed and the reservoir pressure, taking the gas to be in thermodynamic equilibrium. This is done by a computer program known as the ESTC (Equilibrium shock tube calculation). From these reservoir conditions, the nonequilibrium flow through the conical nozzle was then determined using the computer program NENZF (nonequilibrium nozzle flow) based on the method of Lordi et al.[7] for one-dimensional nonequilibrium gas expansions. Extensive measurements by Stalker[8] made in the Shock Tunnel T3 have confirmed that the calculated freestream flow is realized in the test section.

The results have not been corrected for conicity effects of the nozzle. Calculations indicated them to be no more than 10%; consequently, they have not been included.

Models and Instrumentation

An aluminium blunt cone model with a 10-deg half-angle cone and varying nose radii, but common base was used for the experiments. Thus, the effect of nose bluntness, although keeping the cone angle constant, could be studied. The nose radius varied from 3 mm to 25.4 mm giving the bluntness ratio variation R_N/R_B from 0.03 to 0.25. All measuring locations were on the conical skirt of the model and their location varied between $0.878 > x/L > 0.059$ depending upon the model. The model configuration is shown in Fig. 1. During the tests, the model was set at zero incidence and the model wall temperature was taken to be 300 K ambient.

Surface thermocouples to measure heat transfer rates were positioned on the generators of the cone with an angular disposition of 45 deg from each other. The axial locations were chosen such that an adequate resolution of heat transfer distribution over the cone could be obtained (Fig. 2). There were in all eight surface thermocouples but one thermocouple (second from the base, #7, Fig. 2) was found to be unusable because it was found short-circuited before forming a junction. The data, therefore, contain only seven thermocouples.

The surface thermocouples used in these experiments were of the type that have been successfully manufactured and used in the ANU Shock Tunnel Laboratory for some time.[9] The thermocouples are of the chromel/alumel type. They consist of ~0.8-mm wire of one type disposed symmetrically and coaxially into a hollow cylinder of the other whose i.d. and o.d. are 0.84 mm and 1.68 mm respectively. The length of the assembly is ~3 mm. The two thermocouple elements are separated by a thin film of araldite and the whole assembly is electrically insulated from the model by a jacket of heat shrink plastic. The thermocouple junction is formed by gently sanding the end surface of the thermocouple to be exposed to the flow. Observation of the junction surface through a microscope showed that sanding of the thermocouple tip smears fine strands of one material across the gap to make contact with the other. The schematic of the thermocouple assembly is shown in Fig. 3.

Although the thermocouple junction is formed through direct mechanical contact between the two metals, the thermocouples have been shown to be quite robust. In fact, it is not unusual to find them working quite reliably even after about 20–30 shots of the tunnel. This is in marked contrast to thin film gauges, which rarely last more than one or two shots under these high-enthalpy conditions. In addition, it was also found that these thermocouples are less susceptible to ionization effects compared to the thin film gauges. The greater robustness of the thermocouple may be due, in part, to the

lower temperatures attained by the thermocouple junction when exposed to the same flow. This occurs because the thermocouple's metal substrate has a thermal product that is approximately three times that of the substrate most often used for thin film gauges; namely, Macor, Pyrex, glass, and so forth.

A number of subsidiary experiments were conducted to compare the frequency response and output of these thermocouples by placing them side-by-side with a thin film gauge exposing them simultaneously to the same flow and monitoring the response. These experiments showed that the frequency response of the thermocouple, about 100 kHz corner frequency, although lower than that of the thin film gauge, is quite adequate for the duration of steady flow ~600 μs of the shock tunnel.

Computation of Heat Transfer Rates and Data Accuracy

The heat transfer rate in the present experiments is obtained by recording the time history of the surface temperature that is obtained using the thermocouples described above. The thermocouple is treated here as uniform in thermal properties and "semi-infinite" in the direction normal to the surface. The semi-infinite assumption is justified because within the measurement period between 300–700 μs after shock reflection the thermal penetration depth is small compared to the thermocouple dimensions. Then, following Shultz and Jones,[10] the heat transfer is obtained using the relation

$$\dot{q}_w(t_n) = \frac{2}{\sqrt{\pi}} (\rho c k)^{1/2} \left[\sum_{i=1}^{n} \frac{T(t_i) - T(t_{i-1})}{(t_n - t_i)^{1/2} + (t_n - t_{i-1})^{1/2}} \right] \quad (1)$$

This enables us to calculate $\dot{q}_w$ from the temperature trace obtained in real time. The temperature is obtained from the thermocouple output voltage via the temperature coefficient for chromel/alumel of 40 μV/K. The thermal product $(\rho ck)^{1/2}$ was determined by calibration[11] and was found to be 6700 $Ws^{1/2}m^{-2}K^{-1}$. This may be compared with the value of 2004 $Ws^{1/2}m^{-2}K^{-1}$ obtained for the MACOR substrate.[12]

The temperature traces are numerically integrated on a microcomputer after the thermocouple signals are amplified and processed through a LeCroy 2264 waveform digitizer. The amplification and signal recording arrangement is shown in Fig. 4a, and a typical temperature trace in Fig. 4b.

Based on the accuracy of the recording instrumentation (±5%), the variability in the thermocouple output from shot to shot (±6%), and the uncertainty in the value of $(\rho ck)^{1/2}$ (±4.5%), the overall accuracy of heat transfer data is expected to be of the order of ±15%.

Results and Discussion

Blunt Cone Measurements

Figures 5a and 5b show the effect of nose bluntness on cone heat transfer. The abscissa x/L increases from the base toward the nose (see Fig. 1). The heat transfer rates were nondimensionalized with respect to the stagnation heat transfer of a sphere of the same radius as the spherical cap of the cone. This was calculated using the relation given by Sutton and Graves[13] for the equilibrium stagnation heat transfer on a spherical nose in a medium of arbitrary gas mixtures. This relation is

$$\dot{q}_s = K \left(\frac{p_{t2}}{R_N} \right)^{1/2} (h_o - h_w) \quad (2)$$

The proportionality constant K varies depending upon the test gas. It is 0.1113 kg/s $m^{3/2}atm^{1/2}$ for air.

In applying Eq. (2) in the present instance, certain simplifying assumptions have been made. First, in the shock layer at the nose behind the bow shock, the recovery enthalpy h_r is considered to be approximately the same as the freestream stagnation enthalpy h_0. This, of course, assumes equilibrium flow in the shock layer. However, it is possible that a significant proportion of the freestream enthalpy is locked up as frozen chemical enthalpy. If after passing through the shock, the flow in the shock layer remains frozen, then $h_r < h_0$ and the values of $\dot{q}_s$ as obtained from Eq. (2) would be an overestimate.

In order to verify this, the stagnation heat transfer rate was measured on the 25.4 mm radius spherical nose for the highest enthalpy case B and it was found that the experimental value was about 13% lower than that calculated using Eq. (2). However, because there was no provision on other nose radii to measure stagnation point heat transfer, for the sake of consistency, it was decided to use the $\dot{q}_s$ values calculated using Eq. (2). The fact that the measured value on the largest spherical nose yielded less than the equilibrium value [Eq. (2)] could be an indication that the flow in the stagnation region downstream of the bowshock may not still have attained com-

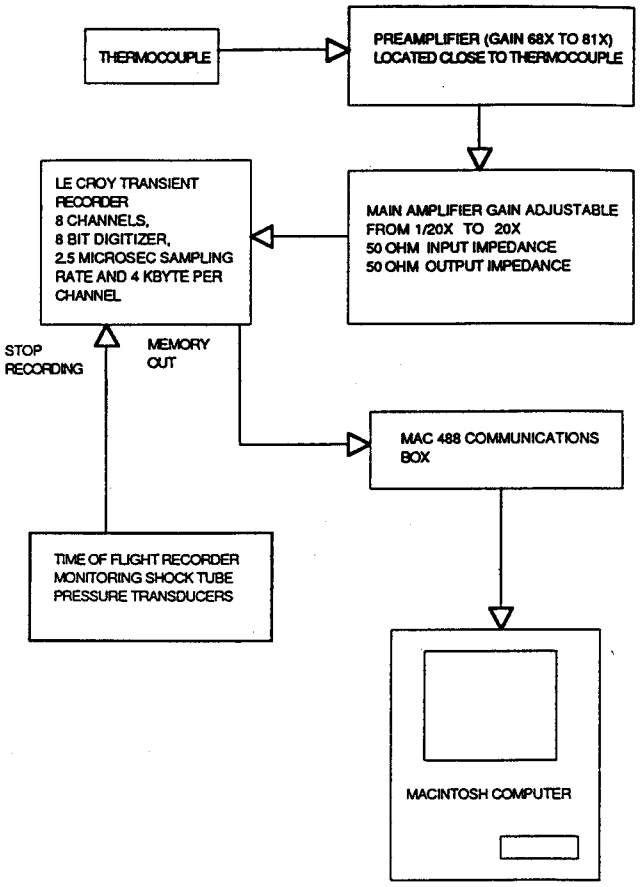

Fig. 4a Schematic of the data acquisition system.

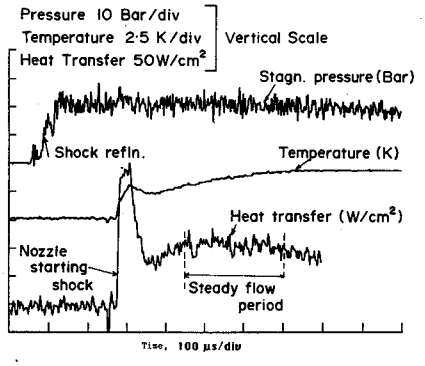

Fig. 4b Typical temperature and heat transfer traces; steady flow is 350 μs (approx.) after the nozzle starting shock.

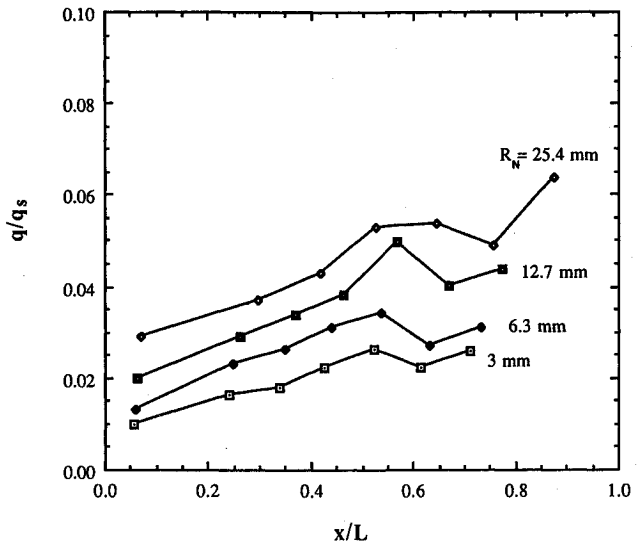

a) Condition "B" (H)

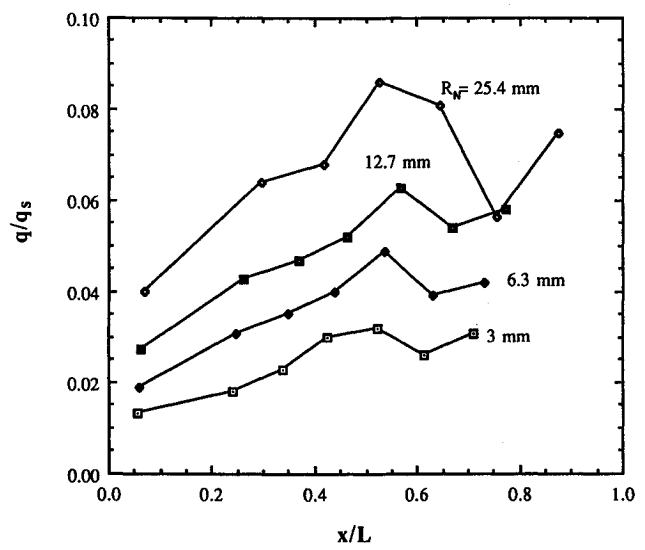

b) Condition "D" (M)

Fig. 5 Effect of nose bluntness on cone heat transfer.

plete chemical equilibrium and this situation may be true for other noses as well.

Returning to measurements on the conical skirt, Figs. 5a and 5b, we note that the nondimensional heat transfer rate increases with increase in the bluntness ratio as expected. We also note that measurements on the aft portion are quite smooth, while those on the forward part especially in the region of sphere/cone junction show some fluctuations particularly for larger bluntness ratios. This is thought to be the result of the bow shock interaction with the nozzle shear layer. As the bow shock interaction with the nozzle shear layer becomes stronger with increase in bluntness ratio, it is reflected as an expansion, which in turn would be incident on the cone and may affect locally, thus reducing heat transfer in that region. This would explain the dip in heat transfer at thermocouple location 2. The measurements were repeated a number of times and the thermocouples were found to be in order. No other explanation seems plausible at present. It may be pointed out that such fluctuations in the region of sphere/cone junction have also been seen by Richards et al.[14] in their measurements of heat transfer distribution on a blunt-nosed model at zero incidence.

Second, heat transfer rates for the lower enthalpy condition D are higher than those for the higher enthalpy condition B. This is to be expected on two counts. First, with condition D, the density is slightly higher. More importantly, increased stagnation enthalpy of condition B increases the level of frozen atomic species in the freestream, which in turn may result in the reduction of heat transfer if the surface behavior is noncatalytic.

A somewhat better correlation is obtained when the results are expressed in terms of the parameter $\dot{q}/\dot{q}_s\sqrt{R_N}$ plotted against the nondimensional distance x'/R_N (Figs. 6a and 6b). The parameter $\dot{q}/\dot{q}_s\sqrt{R_N}$ is, in fact, a variation of the product of freestream-based Stanton number and Reynolds number based on nose radius, and hence should correlate directly with nose radius for a given flow condition, which it seems to do.

Comparison with Theory

Figures 7a, b, c, and d show the experimental data compared to the well-known theory of Lees[1] for convective heat transfer to a blunt cone. Lees' expression is

$$\frac{\dot{q}_w}{\dot{q}_0} = A(\theta_c)\left\{\frac{s'/R_N}{[B(\theta_c) + (s'/R_N)^3]^{1/2}}\right\} \tag{3}$$

where s' is the distance along the surface as measured from the "virtual tip" of the blunt cone and R_N is the nose radius. The parameters $A(\theta_c)$ and $B(\theta_c)$ can be calculated using expressions given by Lees to include real gas effects. Lees'

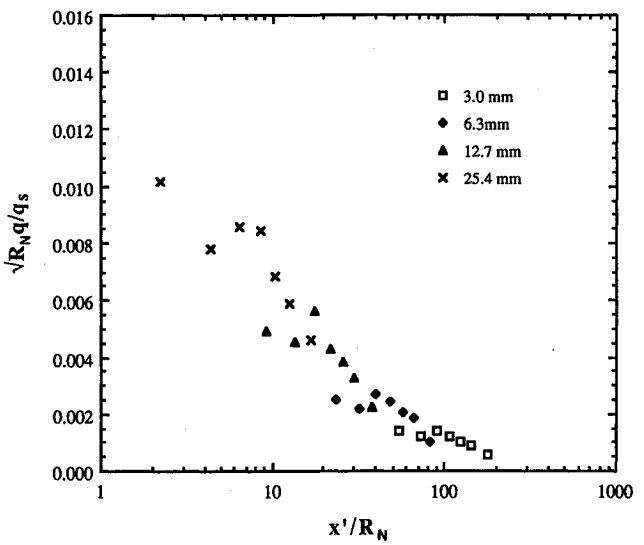

a) Condition "B" (H)

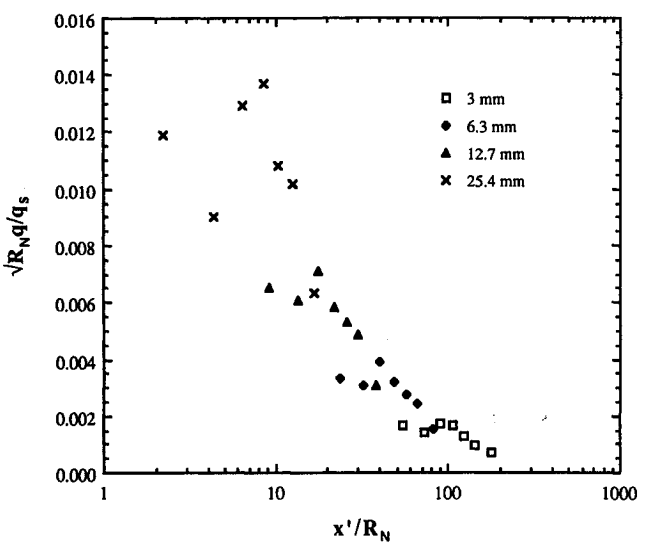

b) Condition "D" (M)

Fig. 6 Correlation of data with $(\dot{q}/\dot{q}_s)\sqrt{R_N}$.

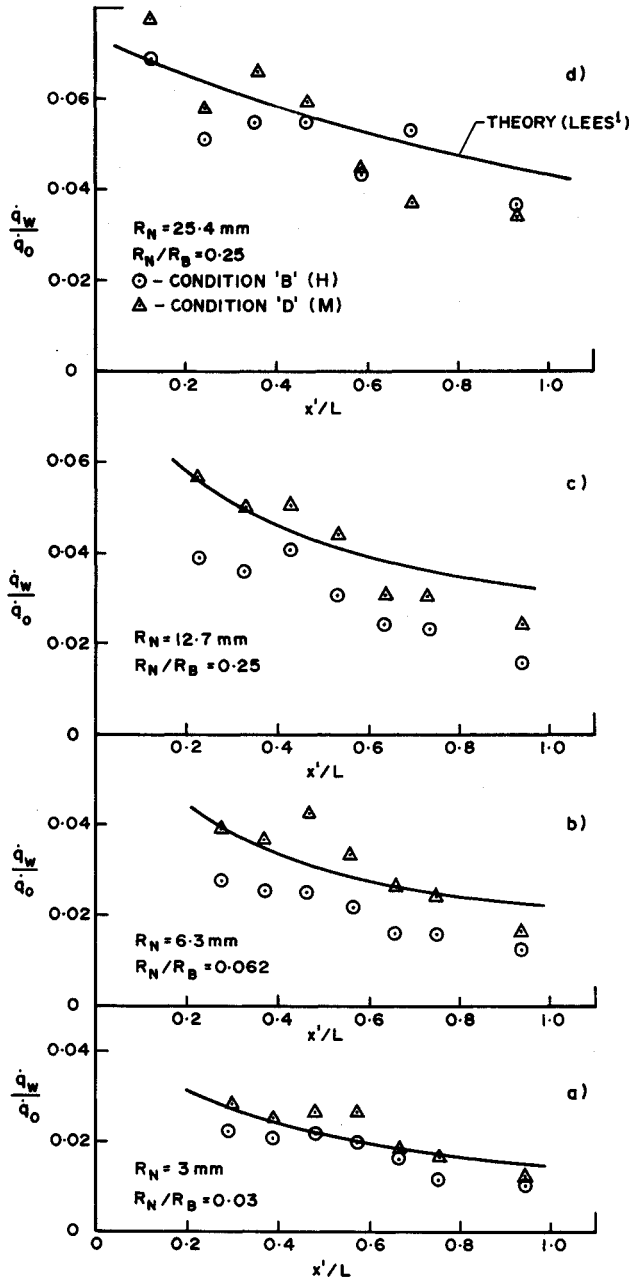

Fig. 7 Comparison of experimental data with Lees' theory.

theory is based on the following assumptions 1) equilibrium conditions prevail in the shock layer; and 2) pressure gradient effect on heat transfer rate is small for cold walls.

Examination of the results shows some interesting features. First, while the agreement with theory with the smallest nose radius seems adequate, results for larger nose radii show considerable scatter. Second, heat transfer rates for condition B are, in general, consistently lower than the theory, while those of condition D seem to be in better agreement with theory, although at some thermocouple locations (particularly 3 and 4), they are consistently higher than the theory. The reason for this is at present unresolved.

Results for all the nose radii are particularly low downstream near the base. This is considered to be due to the upstream influence of the expansion at the base corner and the downstream wake.[5]

It was alluded to in the earlier discussion that the results for condition B are lower than the equilibrium values because of the increased level of frozen atomic species in the freestream with the result that the postshock flow in the immediate vicinity of the nose would be in chemical nonequilibrium. To see this, consider the comparsion between theoretical and experimental heat transfer at the location of thermocouple 4, midway on the cone skirt (Fig. 8). We note that measurements at condition D are nearer to the best line of fit, within the experimental accuracy, while with condition B, they are distinctly away from the line of fit, particularly the measurements with R_N = 6.3 and 12.7 mm. The reason as to why the measurements with R_N = 3 and 25.4 mm, the smallest and the largest nose radius, are close to theory, may be a length-scale effect. For the smallest nose radius, the cone is much longer (L/R_N = 180), so that the flow on the cone skirt has sufficient fetch ahead to attain equilibrium, although the nose radius is much smaller. On the other hand, for the largest nose radius (L/R_N = 17.13) the relaxation length will be much smaller than the nose radius, so that, again, the flow on the cone skirt would tend to attain equilibrium.

Griffith and Lewis[4] measured laminar heating rates on a 9-deg half-angle 0.3 bluntness ratio cone in hot shot tunnels at hypervelocities yielding stagnation temperatures in the range 2800–4000 K. These experiments were conducted using conical nozzles, and temperatures were measured using surface thermocouples. Using modified Cheng's parameter[15] and based on their experimental data and those of CAL,[6] they proposed an empirical relation for the heat transfer on a slender blunted cone

$$\frac{\dot{q}_w}{\dot{q}_0} C \left[\frac{\rho_\infty U_\infty^2}{2p_{o'}}\right]\left(C_p + \frac{2}{\gamma M_\infty^2}\right) \tag{4}$$

valid for Cheng's distance parameter $(x'/d)\theta_c^2/(\varepsilon k)^{1/2}$ in the range 0.05–0.6. They also found that this compares quite favorably with the G.E. real gas (air) characteristics solution.[17]

The largest nose radius cone in the present experiments has a bluntness ratio of 0.25 and θ_c = 10 deg, and as such, is not significantly different from the one used by Griffith and Lewis.[4] Also, for this cone $(x'/d)\theta_c^2/(\varepsilon k)^{1/2}$ varied from 0.076–0.58, and thus was in the range of validity of Eq. (4). Griffith and Lewis[4] also found that when expressed in terms of modified Cheng's[16] parameter, both pressure and heat transfer were independent of Mach number and cone angle.

Therefore, an attempt was made to examine the validity of Eq. (4) for use with the largest nose radius cone. For this purpose, $(\rho_\infty U_\infty^2/2p_{0'})$, γ and the constant C were evaluated for real gas effects. Figure 9 shows the results. We see that the comparison between the empirical relation and the ex-

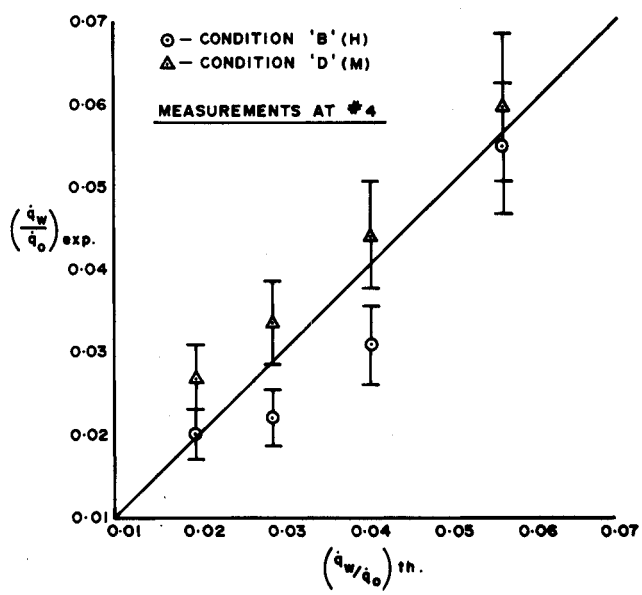

Fig. 8 Comparison between theory and experiment at thermocouple location 4.

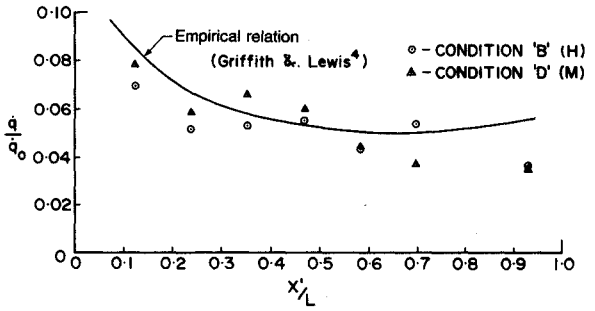

Fig. 9 Comparison of experimental data with the empirical relation of Griffith and Lewis.

perimental data is reasonable. It would seem that the validity of Eq. (4) is fairly general, as long as the measurements are in the range $0.05 < (x'/d\theta_c^2/\varepsilon k)^{1/2} < 0.6$.

Surface Catalycity Effects

Attention was given to possible surface catalycity effects in view of the aluminum surface of the cone skirt. Tests conducted with and without noncatalytic cover (2-μm-thick acrylic lacquer coating on the model) showed no change in heat transfer results. The assumption is, therefore, made that all the data here obtained with noncoated surface pertain to a noncatalytic surface. Also, the gasphase Damkohler number in the boundary layer was calculated using the expression given by East et al.[18] based on the reactions

$$O + O + M \rightarrow O_2 + M \text{ for oxygen}$$

$$N + N + M \rightarrow N_2 + M \text{ for nitrogen}$$

which gave values of the Damkohler numbers of the order of 3.5×10^{-3}, based upon the conditions behind the equilibrium bow shock and assuming the velocity at the edge of the boundary layer on the cone skirt to be approximately the same as the freestream. This suggested that the boundary layer was frozen. Furthermore, extensive heat transfer studies on flat plates in this facility[17,18] have shown that surfaces such as aluminum and steel (SiO_2-coated) were noncatalytic under flow conditions such as these.

Conclusions

Laminar heating rates on cones of various bluntness ratios in high-enthalpy, hypervelocity airflows have been obtained. Flow conditions at the nozzle exit were frozen dissociated. Comparison of the measured data with the well-known theory of Lees[1] showed reasonable agreement for the cone with smallest bluntness ratio. The agreement was not as good for the larger ratios. This is attributed to possible flow nonequilibrium and scale effects. Results for the largest bluntness ratio cone showed reasonable agreement with the empirical relation proposed by Griffith and Lewis[4] for slender, blunt cones.

Acknowledgments

Technical assistance of Ian Darrack and Paul Walsh in operating the T3 facility is appreciated. Thanks are also due to N. R. Mudford for useful discussions and particularly for suggesting the correlating parameter used in Fig. 6.

References

[1]Lees, L., "Laminar Heat Transfer over Blunt-nosed Bodies at Hypersonic Flight Speeds," *Journal of Jet Propulsion*, Vol. 26, 1956, pp. 259–268.

[2]Johnson, R. H., "The Cone Sphere in Hypersonic Helium above Mach 20," *Aerospace Engineering Magazine*, Feb. 1959, pp. 30–34.

[3]Lewis, C. H., "Pressure Distribution and Shock Shape over Blunted Slender Cones at Mach Numbers from 16 to 19," Arnold Engineering Development Center TN-61-81, 1961.

[4]Griffith, B. J., and Lewis, C. H., "Laminar Heat Transfer to Spherically Blunted Cones at Hypersonic Conditions," *AIAA Journal*, Vol. 2, No. 3, 1964, pp. 438–444.

[5]Wittlif, C. E., and Wilson, M. R., "Heat Transfer to Slender Cones in Air Flow including Yaw and Nose-bluntness Effects," *J. Aerospace Sci.*, Vol. 29, No. 7, 1962, pp. 761–774.

[6]Wilkinson, D. B., and Harrington, S. A., "Hypersonic Force, Pressure and Heat Transfer Investigations of Sharp and Blunt Slender Cones," Cornell Aeronautical Lab. Rept., AF-1560-A-5, 1962.

[7]Lordi, J. A., Mates, R. E., and Moselle, J. R., "Computer Program for the Numerical Solution of Non-Equilibrium Expansions of Reacting Gas Mixtures," NASA CR-472, 1966.

[8]Stalker, R. J., "Free-Piston Shock Tunnel T3," *Facility Handbook*, Univ. of Queensland, Australia, 1985.

[9]Mudford, N., private communicaton, 1987.

[10]Schultz, D. L., and Jones, T. V., "Heat Transfer Measurements in Short Duration Facilities," AGARD Rept. 165, 1973.

[11]Barr, A. D., "Investigation of Thermocouples for Use in Shock Tunnels," B.Sc. Honours Thesis, Australia National Univ., Canberra, Australia, Nov. 1988.

[12]Miller, C. G., Micol, J. R., and Gnoffo, P. A., "Laminar Heat Transfer Distributions on Biconics at Incidence in Hypersonic Hyper Velocity Flows," NASA TP-2213, Jan. 1985.

[13]Sutton, J., and Graves, R. A., "A General Stagnation Point Convective Heating Equation for Arbitrary Gas Mixtures," NASA TR-R-376, 1972.

[14]Richards, B. E., Dicristina, V., and Minges, M. L., "Heat Transfer and Pressure Distribution on Sharp and Finite Bluntness Biconic and Hemispherical Geometries and Various Angles of Attack in a Mach 15–20 Flow," Von Karman Inst. TN-71-4, Sept. 1971.

[15]Cheng, H. K., "Hypersonic Flow with Combined Leading Edge Bluntness and Boundary Layer Displacement Effect," Cornell Aeronautical Lab. Rept. AF-1285, A-4, 1960.

[16]Gravals, F. G., Edelfelt, I. H., and Emmons, H. W., "The Supersonic Flow about a Blunt Body of Revolution for Gases at Chemical Equilibrium," General Electric R58SD245, 1958.

[17]East, R. A., Stalker, R. J., and Baird, J. P., "Measurements of Heat Transfer to a Flat Plate in a Dissociated High Enthalpy Laminar Air Flow," *Journal of Fluid Mechanics*, Vol. 97, 1980, pp. 673–699.

[18]Gai, S. L., Reynolds, N. T., Ross, C., and Baird, J. P., "Measurements of Heat Transfer in Separated High Enthalpy Dissociated Laminar Hypersonic Flow Behind a Step," *Journal of Fluid Mechanics*, Vol. 199, 1989, pp. 541–561.